JOURNAL OF GEOPHYSICAL RESEARCH, VOL. 113, A06101, doi:10.1029/2007JA012577, 2008

Predicting interplanetary shock arrivals at Earth, Mars, and Venus: A real-time modeling experiment following the solar flares of 5–14 December 2006

S. M. P. McKenna-Lawlor,[1] M. Dryer,[2,3] C. D. Fry,[2] Z. K. Smith,[3] D. S. Intriligator,[4] W. R. Courtney,[5] C. S. Deehr,[6] W. Sun,[6] K. Kecskemety,[7] K. Kudela,[8] J. Balaz,[8] S. Barabash,[9] Y. Futaana,[9] M. Yamauchi,[9] and R. Lundin[9]

Received 31 May 2007; revised 15 November 2007; accepted 21 February 2008; published 3 June 2008.

[1] A 3-D, kinematic, solar wind model (Hakamada-Akasofu-Fry version 2 (HAFv.2)) is used to predict interplanetary shock arrivals at Venus, Earth, and Mars during a sequence of significant solar events that occurred in the interval 5–14 December 2006. Mars and Venus were on the opposite side of the Sun from Earth during this period. The shocks from the first two east limb events (5 and 6 December) were predicted to interact to form a single disturbance before reaching Earth and Venus. A single shock was indeed recorded at Earth only about 3 h earlier than had been predicted. The composite shock was predicted by HAFv.2 to arrive at Venus on 8 December at ~0500 UT. Solar energetic particles (SEPs) were detected in Venus Express Analyzer of Space Plasmas and Energetic Atoms-4 data for some 3 d (from <0530 UT on 6 December), and an energetic storm particle (ESP) event signaled the arrival of a single shock wave at 0900 UT on 7 December. SEPs were correspondingly recorded at Mars. However, the eastern flank of the composite shock was predicted to decay to an MHD wave prior to reaching this location, and no shock signature was observed in the available data. The shocks generated in association with two flare events that occurred closer to the West Limb on 13 and 14 December were predicted by HAFv.2 to remain separate when they arrived at Earth but to combine thereafter before reaching Mars. Each was expected to decay to MHD waves before reaching Venus, which was at that time located behind the Sun. Separated shocks were observed to arrive at L1 (ACE) only 8 min earlier than and 5.3 h later than their predicted times. The western flank of the combined shocks was predicted to arrive at Mars early on 20 December 2006. An indication of the passage of this shock was provided by a signature of ion heating in Mars Express IMA (ion mass-resolving analyzer) data from <0424 UT on 20 December. The predictions of the HAFv.2 model for Earth were each well within the ±11 h. RMS error earlier found, on the basis of significant statistics, to apply at 1 AU during the rise and maximum phases of solar cycle 23. Overall, the model is demonstrated to be capable of predicting the effects produced by shocks and by the background solar wind at Venus, Earth, and Mars. It is suggested that the continuous presence of solar wind monitors (plasma and interplanetary magnetic field observations) at "benchmark planets" can constitute a necessary and valuable component of ongoing and future space weather programs for the validation of solar wind models such as HAFv.2.

Citation: McKenna-Lawlor, S. M. P., et al. (2008), Predicting interplanetary shock arrivals at Earth, Mars, and Venus: A real-time modeling experiment following the solar flares of 5–14 December 2006, *J. Geophys. Res.*, *113*, A06101, doi:10.1029/2007JA012577.

[1]Space Technology Ireland, National University of Ireland, Maynooth, UK.
[2]Exploration Physics International, Inc., Huntsville, Alabama, USA.
[3]Space Environment Center, Space Weather Predictions Centre, National Weather Agency, NOAA, Boulder, Colorado, USA.
[4]Carmel Research Center, Santa Monica, California, USA.
[5]Space Operations, U.S. Air Force Weather Agency, Offutt Air Force Base, Omaha, Nebraska, USA.
[6]Geophysical Institute, University of Alaska, Fairbanks, Alaska, USA.
[7]Research Institute for Particle and Nuclear Physics, Központi Fizikai Kutató Intézet, Budapest, Hungary.
[8]Institute of Experimental Physics, Kosice, Slovakia.
[9]Swedish Institute of Space Physics, Kiruna, Sweden.

0148-0227/08/2007JA012577$09.00

1. Introduction

[2] NOAA active region 0930 transited the solar east limb (S06, E90) on December 5 2006. It produced four significant X flares and several coronal mass ejections (CMEs) during its disk passage at the beginning of the minimum phase of solar cycle 23. Routine operational predictions of interplanetary (IP) shock arrivals at Earth obtained using the Hakamada-Akasofu-Fry version 2 (HAFv.2) three-dimensional model (section 3.1) were extended to include, in real time, Mars and Venus as ''targets of opportunity.'' We here define ''multibenchmarking'' as the validation of interplanetary shock predictions at multiple planets and/or spacecraft and associatively compare the predictions of the HAFv.2 model with respect to the December 2006 activity with preliminary in situ solar wind plasma and interplanetary magnetic field (IMF) data available from ACE (Advanced Composition Explorer) at L1 and from ion and electron experiments made aboard VEX (Venus Express) and MEX (Mars Express). As will be discussed later, measurements made at VEX and MEX are suggestive of the validation of shock arrival predictions at Venus and Mars. Lack of data acquisition at Mercury requires the available shock predictions of the HAFv.2 model to remain unconfirmed at this planet. We suggest that our experimental approach may be used as a template for both the ongoing and future multibenchmarking validation of models such as HAFv.2.

[3] The benchmarking discussed in this paper is of particular interest because Earth, the base for our solar activity observations, was in the heliospheric hemisphere opposite to that occupied, at the relevant time, by the other planets mentioned above. An important scientific and operational goal is to develop capability to forecast the arrival of solar disturbances at different locations within the heliosphere. Note that we direct attention in this paper to the solar events as they were represented by (fiducial) IP shock arrivals rather than by the occurrence of phenomena such as interplanetary coronal mass ejections (ICMEs).

[4] Multibenchmarking of 3-D solar wind models has already been reported in the literature, and we mention here several pioneering cases. The first comprised an interesting ''problem'' geomagnetic storm that took place in the interval 14–23 April 1994 when a very large polar crown erupted with, presumably, no ''associated'' corotating interaction region (CIR), eruptive prominence or flare [*McAllister et al.*, 1996]. This two-point benchmark modeling attempt combined a 3-D MHD model with a spatial and temporal pressure pulse, suggested by the soft X-ray observations recorded aboard spacecraft Yohkoh, to simulate the resulting ICME/shock propagation to Earth and Ulysses [*Dryer et al.*, 1997]. It is noted that the latter spacecraft was located at that time at a distance of 3.2 AU at S60, E30 relative to the Sun-Earth line.

[5] Another 3-D effort [*Odstrcil et al.*, 1998] was made after a series of 17 major solar flares (classified as M and X) took place from 16 to 23 March 1991. A retrospective SOLTIP (Solar Traveling Interplanetary Phenomena) Interval No. 1 was declared by SCOSTEP (Scientific Committee for Solar Terrestrial Physics). These Intervals constitute the forerunner series of the present CAWSES projects described at http://www.bu.edu/cawses. Four benchmarks were used in this modeling effort: SSCs at Earth, Ulysses, Pioneer-Venus-Orbiter, and Galileo (as in the present case for Mercury, no data were available for comparison with the predictions during the transit of Galileo to Jupiter). Input pulses at 0.1 AU were provided by an empirical procedure on the basis of a flare classification scheme [*Akasofu and Fry*, 1986] and on radio metric type II shock speed estimates [*Smart et al.*, 1984]. *Odstrcil et al.* [1998] indicated that these results were less than satisfactory and noted that the main problem was in choosing ''initialization of interplanetary disturbances because of complex solar activity and observations at different locations.'' These problems persist here, although we hope to demonstrate a modest success with respect to our benchmark cases.

[6] A more straightforward two-point benchmark was successfully demonstrated by *Intriligator et al.* [2005, 2006] with respect to the well known Halloween 2003 solar flare events. Earth and Ulysses (5.2 AU, N58, W80) were again used in this analysis. The correlation coefficients at Earth (28 October to 5 November 2003) and Ulysses (3–28 November 2003) in the comparison between simulated (HAFv.2) and observed solar wind speeds were 0.92 and 0.72, respectively.

[7] It is of interest here to mention the aims of several predictive models that are complementary to HAFv.2. Among these, a three dimensional numerical model which incorporates solar magnetic data and a loss-of-equilibrium mechanism for an erupting flux rope that, on ejection, achieves a maximum speed of 1000 km/s was developed by *Manchester et al.* [2004]. This was used to demonstrate that the shock formed in front of such a rope reaches a fast-mode Mach number >4 and a compression ratio >3 by the time it has traveled a distance of 5 R_s from the solar surface. Related work was presented by *Tsurutani et al.* [2003]. In such a scenario, diffusive shock acceleration can account for the energization of particles to about 10 GeV. The radiation hazard posed to manned/unmanned space systems by energetic particles that are either locally accelerated or trapped in the vicinity of an interplanetary shock and transported with it, is currently a matter of concern. Against this background, detailed 3-D shock simulations were performed by *Manchester et al.* [2004, 2005], *Odstrcil et al.* [2005], and *Wu et al.* [2007] in efforts to understand the structure and evolution of CME driven shocks and their relevance to particle acceleration. Also, *Detman et al.* [2006] developed a Sun to Earth system of coupled models to provide, inter alia, a real-time, 3-D MHD based system to aid the forecasting of geomagnetic activity. The performance of this model is currently under test.

[8] Work is in progress to develop an automated shock identification routine using real time particles and fields data recorded upstream of the Earth to provide warnings of incoming particle accelerating shocks [*Cohen*, 2006]. See an account of the methodology to predict shock arrival times using real time STICS (Suprathermal Ion Composition Spectrometer) observations made aboard the WIND spacecraft [*Posner et al.*, 2004], and also a description of the use of historical electron, proton and alpha particle data measured at ACE to train a neural network to provide real time predictions of shock arrival times at Earth [*Vandegriff et al.*, 2005]. Only fragmented as opposed to comprehensive models of solar energetic particles (SEPs) are presently

Table 1. Inputs for the Solar-Terrestrial Events of 5–17 December 2006[a]

Event	FF	Solar Event Date			Time,	Lat.,	Long.,	V_s,	Tau,	V_{sw},			Peak,	End,		
		Year	Month	Day	UT	degrees	degrees	k/s	hmm	k/s	Opt.	X Ray	UT	UT	Sta.	S/C
1	663	2006	12	5	1034	S07	E79	836	157	300	2N	X9	1035	1215	SVI	GOES 12
2	664	2006	12	6	1842	S05	E64	2000	100	525	3B	X6.5	1850	1854	S/W	GOES 12
3	665	2006	12	13	0227	S06	W23	1600	300	650	4B	X3.4	0249	255	CUL	GOES 12
4	666	2006	12	14	2210	S06	W46	1500	200	900	2B	X1.5	2217	2222	CUL	GOES 12

[a]Time, start of the metric type II burst; FF, fearless forecast number (see text); Lat. and Long., from optical data/images of the solar disk; V_s, the near-Sun shock velocity determined from metric type II data; Tau, duration of solar event (determined from soft X ray data); V_{sw}, solar wind speed at 1 AU (from ACE spacecraft data); Opt., optical classification of the flare (where N is normal and B is bright); X ray, classification of the flare in soft X rays (1–8 Å); Sta., station that provided the radio data (SVI, San Vito; S/W, STEREO/WAVES; Cul, Culgoora); S/C, spacecraft that provided the soft X-ray data.

available to explain such key processes as initiation, acceleration and propagation. However, a methodology to amalgamate the existing body of scientific knowledge with empirical data and current engineering models in order to develop an International Standard Model or models of the solar energetic particle environment [cf. also *Smith*, 2002; *Aran et al.*, 2006] can already be foreseen [*Gabriel*, 2006].

[9] The present paper provides a further example of multipoint benchmarking involving HAFv.2 forecasting of shock arrivals at Earth (L1) and at two other inner heliospheric planets. We describe the solar events and Earth-based observations concerned in section 2. The HAFv.2 model and its validations at L1 are described in section 3.1. Validation of HAFv.2 predictions by observations made at

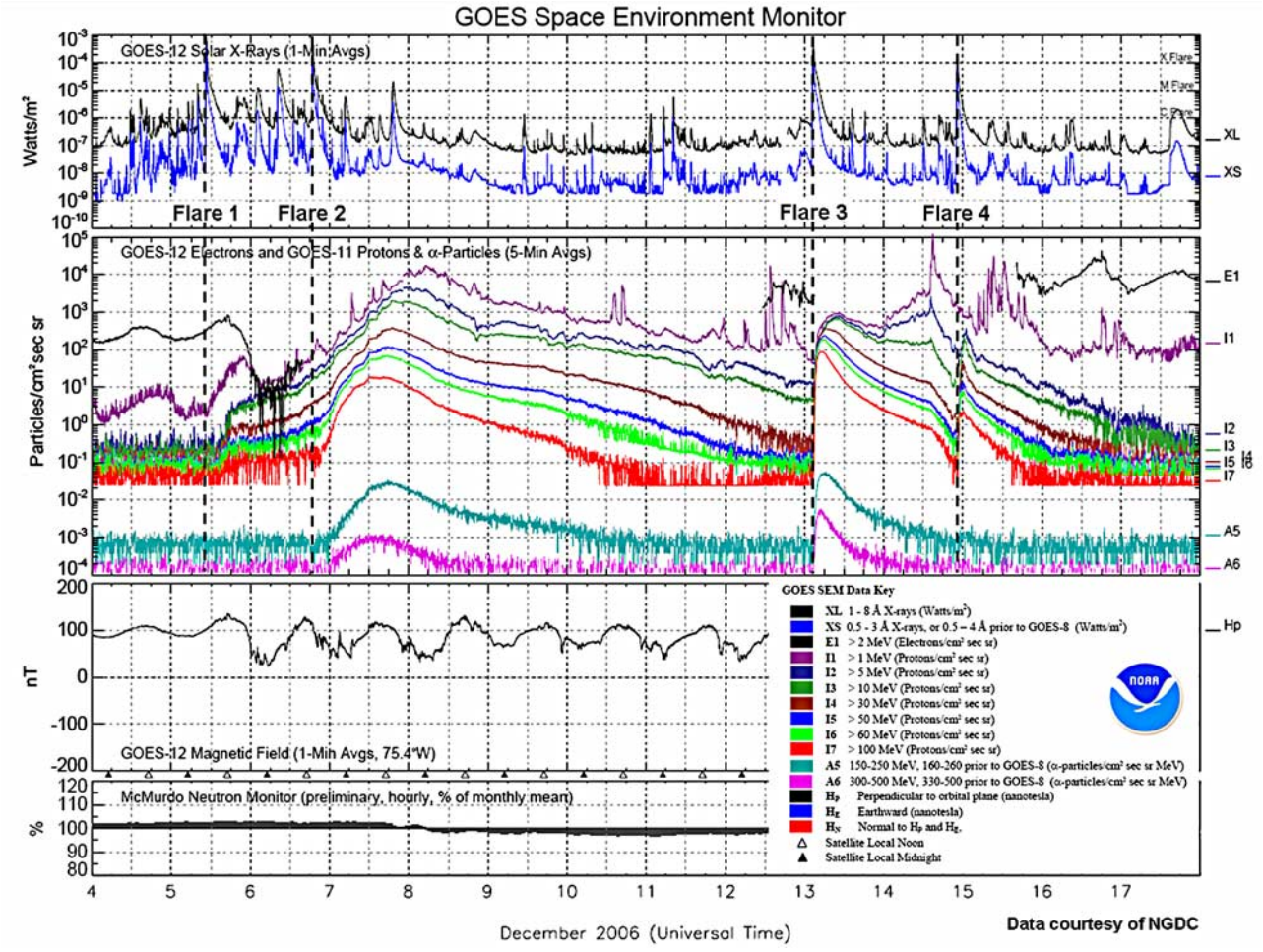

Figure 1. (first panel) GOES 12 soft X-ray fluxes and (second panel) GOES 11 electron and GOES 12 proton and alpha particle fluxes from 5 to 18 December 2006. (third and fourth panels) Also shown are IMF and neutron monitor data. Further details concerning four X class flares (i.e., FF #663, FF #664, FF #665, and FF #666) are given in Table 1. Dashed vertical lines indicate the approximate start times of each flare. Note the ~4.5 h delay until the rapid (unusual for an east limb event) arrival of energetic protons at GOES 11. See text for a possible physical explanation for the fast and subsequent gradual SEP event.

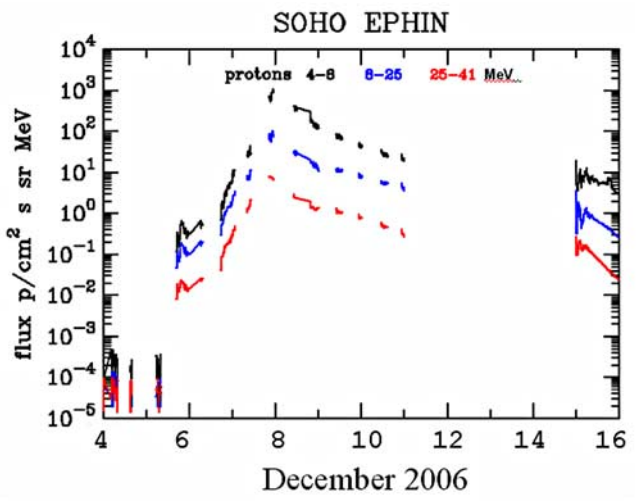

Figure 2. SOHO/EPHIN energetic proton flux from 4 to 16 December 2006. An ESP from the simulated composite shock S1-S2 is seen on 8 December 2006. The large data gap is due to scheduled spacecraft maintenance.

Venus and Mars are discussed in section 3.2. Concluding remarks are offered in section 4.

2. Solar Events

[10] NOAA active region 0930, after several months of low solar activity, transited the solar east limb on 5 December 2006 at S07, E79. Four X class flares took place (see Table 1) during the following 9 d, followed by another prolonged period of low solar activity at the start of the minimum phase of solar cycle 23. The production of these four significant solar flares, an episode of unexpected, east limb related, energetic particle fluxes, and a series of CMEs provide the backdrop for our "three-point" benchmarking experiment.

[11] The first two X flares (5 December (X9/2N, S07,E79 at 1034 UT) and 6 December (X6.5/3B, S05,E64 at 1842 UT)) are illustrated in Figure 1 (first panel) via their accompanying GOES 12 soft X-ray flux profiles. See also Table 1. (We will not consider several C and M class flares that occurred in the same active region in our modeling experiment because no radio metric type II shocks were observed in association with them.)

[12] Figure 1 (second panel) also shows the unusual proton flux responses at GOES 11 in its >1–>300 MeV channels that followed the two (close to the) east limb flares. Figure 2 provides complementary energetic particle fluxes recorded by the Solar and Heliospheric Observatory (SOHO) Electron, Proton, Helium Instrument (EPHIN) at L1 in association with the particle events of 6–7 December. A rapid rise in relatively high-energy particle counts started at about 1500 UT on 5 December, presumably from the flare/CME site, followed by the initiation of a gradual rise that started at about 1800 UT (see also the ACE/EPAM data set in Figure 3). This SEP was supplemented by a further SEP from the second flare that continued over the next few days. The gradual component that followed the second X class flare shows energy dispersion that implies a second particle injection. We will suggest (in section 3) that the HAFv.2-modeled shocks may elucidate the nature of these latter observations, similar instances of which may potentially be seen again in the future in association with very strong, east limb, solar-generated IP shocks.

[13] The SXI (Soft X-ray Imager on GOES 12) recorded an X-ray wave (S. Hill and V. Pizzo, private communication, 2007) which traveled from the E79 flare site, starting at 1034 UT on 5 December, and reached W90 by ~1200 UT on the same day. We interpret this wave to represent the low coronal extension or "skirt" of the interplanetary shock simulated by HAFv.2 that is discussed in section 3. The second flare at E64 on 6 December was followed by a powerful Hα Moreton wave (K. S. Balasubramanian, private communication, 2007). See also the Website of the National Solar Observatory (http://www.nso.edu/press/tsunami) which presents additional evidence of this rapid wave propagation to western longitudes.

[14] The second shock and its Moreton wave skirt combined with the first shock and continued to make connection with Earth as indicated by an increase observed in the slope

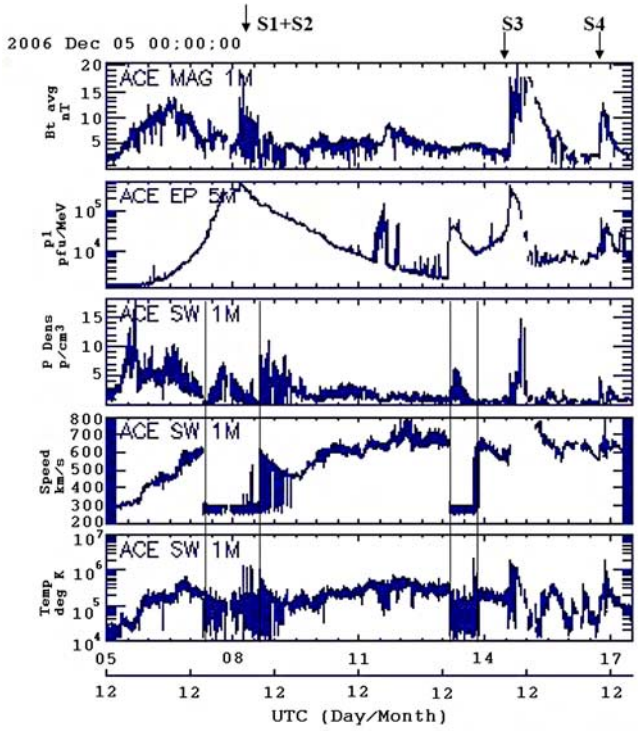

Figure 3. Level 1 data of the ACE/MAG, EPAM, and SWEPAM instruments from 5 to 17 December 2006. One and five min averages (indicated by 1M and 5M, respectively) are indicated on each data set. Note that SWEPAM solar wind proton data are unreliable from ~0700 UT on 7 December until ~1600 UT on 8 December and, again, from ~1340 to ~1800 UT on 13 December. The times of these effectively "down periods" which are marked by pairs of solid vertical lines, were due to the bombardment of the spacecraft by highly energetic protons "snow storm effect" associated with Flares 2 and 3 and their approaching shocks (S2 and S3). The arrival times of composite shock S1-S2 and shocks S3 and S4 are indicated at the top.

Table 2. Comparison of Predicted and Observed Shock Arrivals at 1 AU[a]

		Date HAF – Prediction				Observed at SOHO[b]			Observed at ACE[c]			ΔT,	TT,
Event	FF	Year	Month	Day	UT	Month	Day	UT	Month	Day	UT	h	h
1	663	2006	12	9	1200	...	...	...	...	...	...	Int.[d]	...
2	664	2006	12	7	0800	12	8	0411	12	8	0411	−20	33
3	665	2006	12	14	1400	12	14	1356	12	14	1352	0	35
4	666	2006	12	16	1200	12	16	1722	12	16	1721	−5	43

[a]FF, fearless forecast number (see text); ΔT, shock arrival time predicted by HAFv.2 minus observed arrival time; *TT*, shock arrival time minus start time of metric type II burst.
[b]Observed from Shockspot (SOHO MTOF available at http://umtof.umd.edu/pm/).
[c]Observed at ACE by MAG, EPAM, and SWEPAM (SWEPAM was not available for event 2).
[d]Int., shock interacts and combines with following event to form one wave.

of the flux curve (Figure 1). Finally, with respect to Earth, the energetic storm particle (ESP) flux peak seen in Figure 2 indicates the arrival of the composite shock at SOHO/EPHIN. We speculate on the basis of this suggested scenario that the rapid rise phase at 1500 UT on 5 December, followed by a gradual phase, was initiated by initial westward extension of the IMF connections to Earth of the first shock wave followed by connection of the composite shock to Earth. Further analysis of this suggestion is beyond the scope of the present paper and awaits further study.

[15] The second set of two X flares (13 December (X3.4/4B, S06,W23 at 0227 UT) and 14 December (X1.5/2B, S06,W46 at 2210 UT)) are represented in Figure 1 (first panel) via their GOES 12 soft X-ray flux profiles. Figure 1 (second panel) also shows the prompt and gradual SEP proton fluxes from these two, magnetically well-connected, flares and their associated interplanetary shocks.

[16] The ACE/EPAM (Electron, Proton, and Alpha Monitor) instrument provided energetic proton flux data in several of its channels (ranging from 47 keV to 4.75 MeV) over the entire period 5–17 December 2006. Figure 3 presents part of these data (47–65 keV) in the second panel from the top. The first data set displays the total IMF magnitude measured by the ACE/MAG (magnetometer) instrument. The bottom three data sets provide, respectively, the real time (level 1) solar wind proton density, speed and temperature. We note that the latter three physical parameters are not reliable between ~0700 UT on 7 December 2006 and ~1600 UT on 8 December 2006 and, again, from ~1340–1800 UT on 13 December 2006 (these intervals are contained within the two pairs of vertical lines on the diagram.). These uncertainties are due to temporary energetic particle contamination of the records due to the presence in the spacecraft environment of extremely high-energy proton fluxes associated with Flares 2 and 3. The times of the associated IP shock arrivals at Earth are labeled S1-S2, S3, and S4 at the top and corresponding details are given in Table 2. These shocks are discussed in section 3.

3. Real-Time HAFv.2 Model Predictions of Shock Arrivals at Earth, Venus, and Mars and Their Comparison With Available In Situ Data

[17] We first briefly discuss in sections 3.1 and 3.2 the HAFv.2 model and its three-point December 2006 benchmarking simulation. Details of the origin and development of this model are given by *Hakamada and Akasofu* [1982] and *Fry* [1985], therefore, only a brief overview is provided below. An account of the use of the model in the present context follows, together with a description of its comparison with in situ data, where these are available, at L1 (essentially at Earth.) We then discuss, in section 3.3, the model predictions and observations at Venus and Mars.

3.1. HAFv.2 Model

[18] The HAFv.2 model provides forecasts of both the "quiet" and "event-driven" solar wind. An extensive record of its utilization for shock predictive purposes at Earth is given by *Fry et al.* [2001, 2003, 2004, 2005, 2007], *Smith et al.* [2003, 2004, 2005], *Sun et al.* [2002a, 2002b, 2003], *McKenna-Lawlor et al.* [2002, 2006], and *Dryer et al.* [2001, 2004]. Both real-time and retrospective periods are considered in these works. A root mean square error, RMS = ±11 h. for "hits" at Earth, was determined in an extensive statistical test [*McKenna-Lawlor et al.*, 2006] of real-time forecasts of shock arrival times during the rise and maximum phases of solar cycle 23. It is not presently known if this root mean square error differed during the declining phase of the cycle. The extension of this statistical metric through including an additional 220 events (to January 2007) recorded during the decline of this cycle is a work in progress (Z. K. Smith, private communication, 2007). The HAFv.2 model was also successfully used [*McKenna-Lawlor et al.*, 2005] to "predict" (ex post facto) shock arrivals at Mars and to introduce related preliminary IMF field line and SEP/ESP analysis procedures pertaining to data recorded by the SLED instrument aboard Phobos-2 during orbits of Mars in March 1989.

[19] The modified kinematic approach implemented in HAFv.2 is based upon several guiding assumptions, as described by *Hakamada and Akasofu* [1982] and *Fry* [1985]. The kinematic model ingests radial solar wind speed and radial IMF at 5 R_s. This information was obtained in the present study from SSCS (source current surface sheet) maps provided by a procedure developed by *Wang and Sheeley* [1990] and extended by *Arge and Pizzo* [2000]. This empirical procedure is known by the acronym WSA (Wang-Sheeley-Arge). The WSA algorithm uses daily magnetograms from Mount Wilson Solar Observatory on a 5° × 5° grid in heliolatitude and heliolongitude and provides radial values of the solar wind speed and field strength at the 5 R_s source surface. HAFv.2 uses these values with the same grid size as inputs. Thus, the spatial distribution of solar wind speed and radial IMF is nonuniform on the inner boundary.

[20] As already indicated above, the solar wind is assumed to flow outward from the Sun in a radial direction from the source surface at 5 solar radii. The radial speed has an inhomogeneous distribution on this inner boundary, with higher speeds representing the source of the fast solar wind (e.g., coronal holes) and lower speeds representing the slow wind from regions near the magnetic neutral line (e.g., helmet streamers). The Source Surface maps from NOAA SWPC provide solar wind speeds as gridded fields of magnetic field strength together with an accompanying flux tube divergence factor (α). The radial speed at the inner boundary is computed from such divergence factors to establish the quasi-steady state flows using the equation

$$V_{ss}(\theta, \phi) = V_0 + V_1 \alpha(\theta, \phi)^{-\beta},$$

where $V_{ss}(\theta, \phi)$ is the speed at the inner boundary at a given heliolatitude, θ, and heliolongitude, ϕ; V_0 sets the minimum speed and V_1 is a speed scaling factor. V_0, V_1, and β are constants determined empirically from comparisons of the simulation results with observations at L1. Faster and slower fluid parcels are emitted along each radial as the Sun rotates underneath. Then, the distance, R, traveled along a radial at time, t, is $R = Vt$. By plotting the radial distance that the parcel attains versus the time (t, its age) that the parcel left the Sun, one obtains an *R-t* diagram. The positions of the parcels as a function of time form a curve. If all of the fluid parcels had the same speed, the slope of the curve on the *R-t* diagram would be constant, i.e., a straight line. However, because the speeds are different, the curve on the *R-t* diagram will have peaks and troughs.

[21] The interaction of the fast and slow speed streams is accounted for in a two-step process. First, the faster speed streams are decelerated, and the slower speed streams are accelerated, which has the effect of lowering the peaks and raising the troughs on the *R-t* diagram curve. This step is described by *Hakamada and Akasofu* [1982, equation (3)], which, after correcting for a typographical error in the first term, is given by

$$R = Vt - V_{ss}F(t)G(t)t + V_{ss}F(t)t,$$

where V_{ss} is the speed of the parcel when it left the inner boundary on the source surface at time $t = 0$, and

$$F(t) = Ae^{-(t/\tau_1)} + B,$$

$$G(t) = Ae^{-(t/\tau_2)} + B.$$

A, B, τ_1, and τ_2 in the last two equations are coefficients that were adjusted to provide the best fit of the simulated solar wind parameters with observations made aboard IMP-8 [*Fry*, 1985; *Sun et al.*, 1985]. Minor ad hoc adjustments have been made in the interim to suit changing solar cycle conditions (C. D. Fry, private communication, 2007).

[22] Second, the fluid parcel positions are adjusted so that no parcel overtakes its slower predecessor along a radial. Radial speed at a given distance, R, from the Sun along a radial is computed using *R-t* diagrams at successive time steps, where $V = \Delta R/\Delta T$. The magnetic field is carried along with the flow under the frozen field condition, and field strength and direction are calculated from magnetic flux conservation. Mass flux conservation is used to compute density.

[23] The procedures described allow the model to simulate, to first order, a number of solar wind observations, including the establishment and interaction of fast and slow solar wind stream flow, the development of corotating interaction regions, and the formation of forward/reverse shock pairs. The internal free parameters used are the coefficients in the source surface velocity equation and the acceleration/deceleration equations. These internal parameters, which are fixed and not varied during each event, were originally calibrated [*Sun et al.*, 1985] by comparing the simulations with observations and with 1-D MHD solution results. It is possible that these calibrations would change through more detailed comparisons with 3-D MHD modeling but it is not presently known if this would be the case. Meanwhile, it is noted that the nonuniform, 3-D, quasi-steady state flow is changed, in the present methodology, on a daily basis, because this is necessary for real-time operational use. Contemporaneous flow cannot be provided by the solar minimum bimodal configurations used in some theoretical models (c.f., the account by *Manchester et al.* [2004]).

[24] The process of the initialization of shocks is described by *Hakamada and Akasofu* [1982], section 2.2. The speed V_F on the inner boundary is increased exponentially, governed by an unnumbered equation which, after correcting for a typographical error, is given by, $V_F = V_c(t/\tau)e^{-(t/\tau)}$, where V_F is the speed due to the energy release during the solar event at time, t, τ (tau in Table 1) is the piston driving time of the shock. V_c is the peak speed of the disturbance at the point of energy release on the source surface. V_F on the inner boundary falls off exponentially in latitude and longitude away from the source of the disturbance.

[25] This initialization process affects the strength, speed and transit time of shocks to Earth, Mars, etc. The simulated shock shape is nonspherical, being faster at the nose of the shock and slower on its flanks. Therefore, the transit time of the shock to the observer is affected by the relative longitude of the observer with respect to the heliolongitude of the parent solar event. Higher initial speeds of the shocks at the Sun result in stronger and faster shocks. The interaction of a shock with the preexisting solar wind through which it travels affects the timing, strength and longitudinal extent of the shock propagation. For several examples of the effect of initial shock speed, source longitude and piston driving time on shock arrival timing, the reader is referred to Figures 2 and 4 and a related discussion by *McKenna-Lawlor et al.* [2006]. This topic has also been examined in a parametric 3-D MHD study [*Wu et al.*, 2005] that included various initial shock speeds and variable background solar wind speeds. They found that, for a sufficiently large momentum input "the shock arrival time at Earth is not significantly affected by the preexisting solar wind speed." Additional 1.5-D MHD studies were made for several Halloween, 2003 events [*Wu et al.*, 2006] that included interacting shocks. They found, for example, that the solar wind speed might increase by about 25% after two shocks collide with each other.

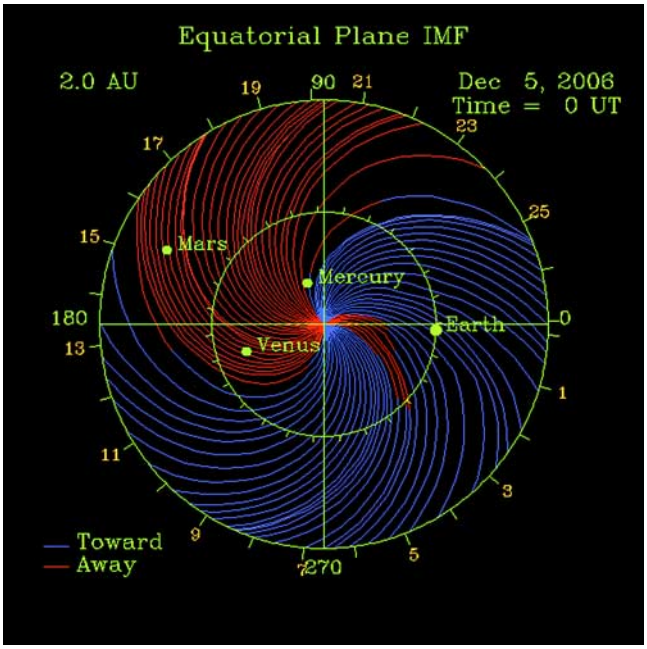

Figure 4. HAFv.2 simulation of the preevent IMF field lines in the ecliptic plane (from the Sun to 2 AU) at 0000 UT on 5 December 2006. "Away" field lines are colored red; "toward" field lines are blue. The inner planets are labeled and shown as solid dots. See the text for an explanation of the numbers on the outer 2 AU circle.

3.2. Three-Point Benchmarking Scenario With Respect to the December 2006 Activity

[26] The account given above is concerned with the basic development of the HAFv.2 model. We now consider our simulation of shock propagation using this tool in the circumstances pertaining during December 2006. Figure 4 shows an ecliptic plane view of the "background" solar wind IMF as simulated by the HAFv.2 model at 0000 UT on 5 December 2006. "Toward" field lines are depicted as blue; "away" lines as red. The positions of the inner planets at this time are represented by dots. The two circles show the respective locations of 1 and 2 AU. Numbers on the outer circle indicate, for an assumed solid rotation of this IMF pattern, the number of days required for the "fixed" configuration (at a given number and along its radius) to reach Earth. For example, the CIR (indicated by closely bunched red IMF lines) about to pass Venus and Mars is predicted to reach Earth in about 14 d. This procedure of course assumes solid body rotation and the ongoing availability of highly accurate line-of-sight magnetograms to implement the WSA procedure.

[27] The tranquil scenario described above was interrupted by Flare 1 on 5 December, see Table 1, followed by the other flares listed therein. HAFv.2 associatively changed to an event-driven mode. Proxy physical characteristics were input at the 5Rs source surface to mimic significant drivers of the ensuing interplanetary disturbances. These input characteristics (for details, see Table 1) were as follows:

[28] 1. Date, time, and disk location of the parent solar event (Hα or GOES/SXI flare location).

[29] 2. Shock start time (generally close to the time of the soft X-ray maximum) determined from the start times of metric type II radio frequency drifts.

[30] 3. Initial coronal shock speed, V_s, based on the type II frequency drift rate and an assumed coronal density model (here: one times the model of *Newkirk* [1961]). The speed is either assumed to be that directly above the radial position of the flare, or an heuristic use is made of the plane-of-sky speed of a CME to represent the shock speed).

[31] 4. Event duration tau. This time is estimated using the soft X-ray profile as a proxy for the piston-driving time of the shock (the full width at half maximum measured linearly on the log plot from just above the preevent background flux level). After this, the entire ICME and the dynamics of its shock are a function of upstream nonuniformity or of interaction with prior ICMEs.

[32] Table 1 also lists the "fearless forecast" numbers, FF. The term fearless forecast was used whenever solar events characterized by the four characteristics listed above were reported in real time to the Boulder Space Environment Center during solar cycle 23. These data were then utilized by dedicated forecasters as inputs to the HAFv.2 model, and the resulting near real time predictions obtained were distributed immediately thereafter, under their individual FF numbers, via an email subscription list.

[33] The background solar wind speed, V_{sw} (although not used by HAFv.2), is also listed at the time of each flare in order to provide a representative snapshot of the flow speed at Earth at that time (i.e., to indicate whether quiet coronal hole high-speed flow pertained or if the prevailing conditions were related to a preceding transient event). The flare classifications; peak and "official" end times of each flare; the identities of the various radio observatories and of the spacecraft making the X-ray measurements are listed in the remaining columns of Table 1. In the present scenario, one deviation from the procedure of item 3 (from the above list) is made in the case of Flare 2. The metric type II speed, reported from Palehua on this occasion, was 827 km/sec. This value was compared with a preliminary value, 2000 km/sec, reported (M. Kaiser, private communication, 2006) from the STEREO/WAVES decametric (10 to 1 MHz) type II observations (fundamental and harmonic) in near real time. In view of the extreme nature of Flare 2 (FF #664) and of its particle characteristics (see above), a subjective decision was made to adopt V_s = 2000 km/sec (rather than the slower metric estimate) in the HAFv.2 initialization procedure.

[34] It may, justifiably, be asked if the "event parameters" listed above are the appropriate ones to use. For example, no consideration was given in the HAFv.2 model to: sigmoids, flux ropes (magnetic clouds), or to situations characterized by "loss of equilibrium" associated with kink instabilities. This is because it is not apparent which observables should best be utilized at event initiation. *Dryer* [1998, 2007] argued that there is at the present time little choice of useable observables to solve the deterministic, classical, initial boundary value problem. This point is especially valid for operational purposes. Further arguments, pro or con, are beyond the scope of the present paper.

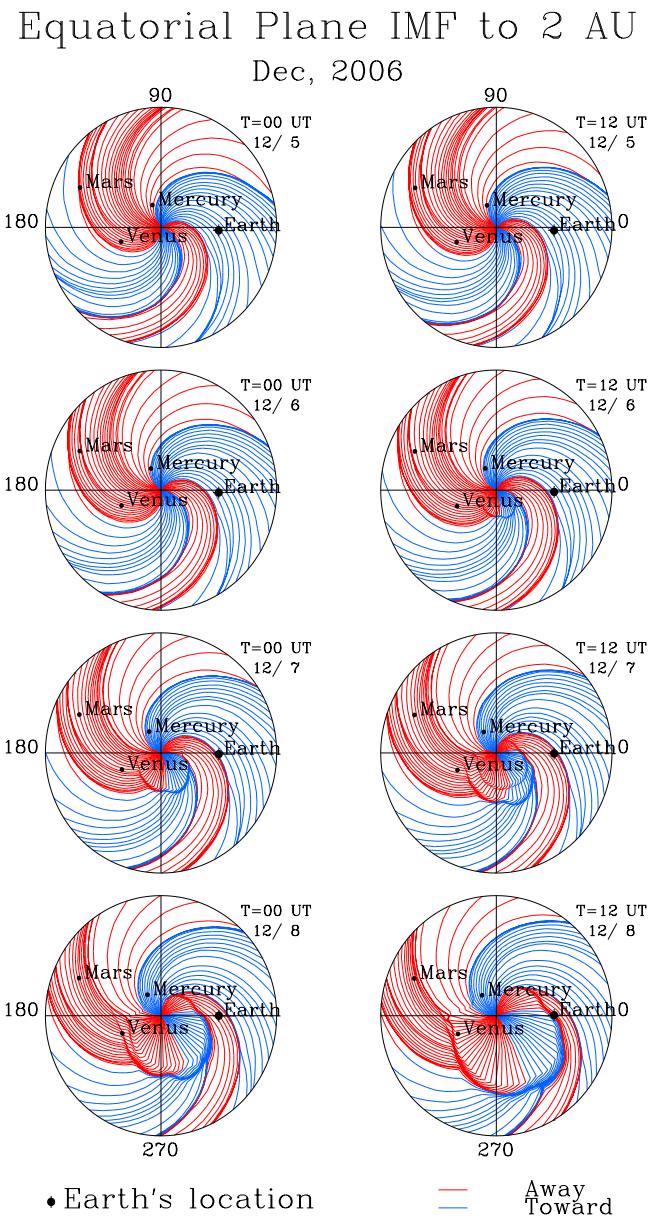

Figure 5. HAFv.2 simulation of disturbed IMF field lines in the ecliptic plane to 2 AU from 0000 UT on 5 December 2006 to 1200 UT on 8 December 2006 subsequent to flares 1 and 2. Shocks 1 and 2 and their eventual composite shock are shown in the lower frames for 6–8 December 2006. The frames have a 12 h cadence.

[35] Figure 5 shows a sequence of ecliptic plane IMF plots of the simulated propagation of shocks (S1 and S2) from the first and second events, namely FF #663 and FF #664. S1 expanded rapidly around the Sun (as also suggested by the observation, discussed in section 2, of a rapidly moving SXI wave skirt). This rapid expansion is illustrated in the 0000 UT, 6 December, frame of Figure 5. It is recalled (section 2) that the SXI wave reached W90 by ~1200 UT on 5 December. Thus, it seems highly probable that the simulated shock easily achieved IMF connection with Earth at about 1800 UT on 5 December.

[36] The second, more powerful shock S2 is seen in the simulation to have caught up with and interacted with S1. During the very early stages of S2, as it refracted around and expanded westward close to the Sun, it is seen (lower four frames in Figure 5) to have intersected IMF lines that connected with Earth. We suggest that the weakened skirt of the actual shock was the Hα Moreton wave discussed in section 2. We also suggest that this early connection provided rapid and ready access to Earth of the strong S2 (and, thereafter, S1-S2 combined and energized the proton fluxes plotted in Figures 1 and 2). Figure 1 shows that the slope of the higher-energy protons making up the SEP increased at about the time of the second flare. This implies increased effectiveness in proton energization at the time of composite shock arrival at the Earth, as is indicated also in the 0000 and 1200 UT simulations of 7 December (Figure 5). The position on the shock where proton energization takes place is referred to as the Connection with Observer (COB) point [*Lario et al.*, 1998; *Aran et al.*, 2007, and references therein]. We suggest that the same physical process occurred along the eastern as well as along the western flanks of the combined shock S1-S2 from Flares 1 and 2. As time advanced, Figure 5 shows that the HAFv.2 model predicted the arrival at Earth of the western flank of merged shock S1-S2 at about 0700 UT on 8 December (see also Table 2). Both ACE/MAG and SOHO/MTOF (Mass Time-Of-Flight) recorded the arrival of this composite shock some 3 h earlier at ~0411 UT on 8 December 2006 after a 33 h transit time following Flare 2 (FF #664). SOHO/EPHIN also detected the ESP peak during shock arrival as shown in Figure 2.

[37] Figure 6 (like Figure 5) shows the sequence of ecliptic plane IMF plots providing the simulated propagation of the third and fourth shocks, S3 and S4, from their associated Flares 3 and 4 (FF #665 and FF #666). These well connected flare locations indicate the IMF pathways to Earth for the SEPs represented in Figure 3. Shock 3 arrived at L1 and was observed by ACE/SWEPAM (Solar Wind Electron, Proton, and Alpha Monitor) MAG at 1352 UT, on 14 December, while S4 arrived at 1721 UT on 16 December 2006. As noted in Table 2, the HAFv.2 model hits were, respectively, within 8 min (listed as 0 h) and −5 h of the measured arrivals after 35 and 43 h transit times (TT) from the Sun.

3.3. HAFv.2 Predictions and Observations at Venus and Mars

[38] We do not have any in situ observations at Mercury. Thus, we can only speculate what its contribution might have been during the epoch discussed to our benchmarking of the HAFv.2 model predictions. We note, however, that in future relevant measurements can be made at Mercury. The Messenger spacecraft has already made its first flyby of the planet, with orbit insertion scheduled for 2011. The Bepi-Columbo mission to Mercury is scheduled for launch in 2014 while the launches of Solar Probe and Sentinels are expected to occur in the same general time frame.

[39] Aboard the Mars Express (MEX) and Venus Express (VEX) spacecraft that are presently in orbit about Mars and Venus are similar suites of four instruments collectively called ASPERA (Analyzer of Space Plasmas and Energetic Atoms). In the present paper we will consider data recorded at each planet by the ASPERA/IMA (Ion Mass-Resolving

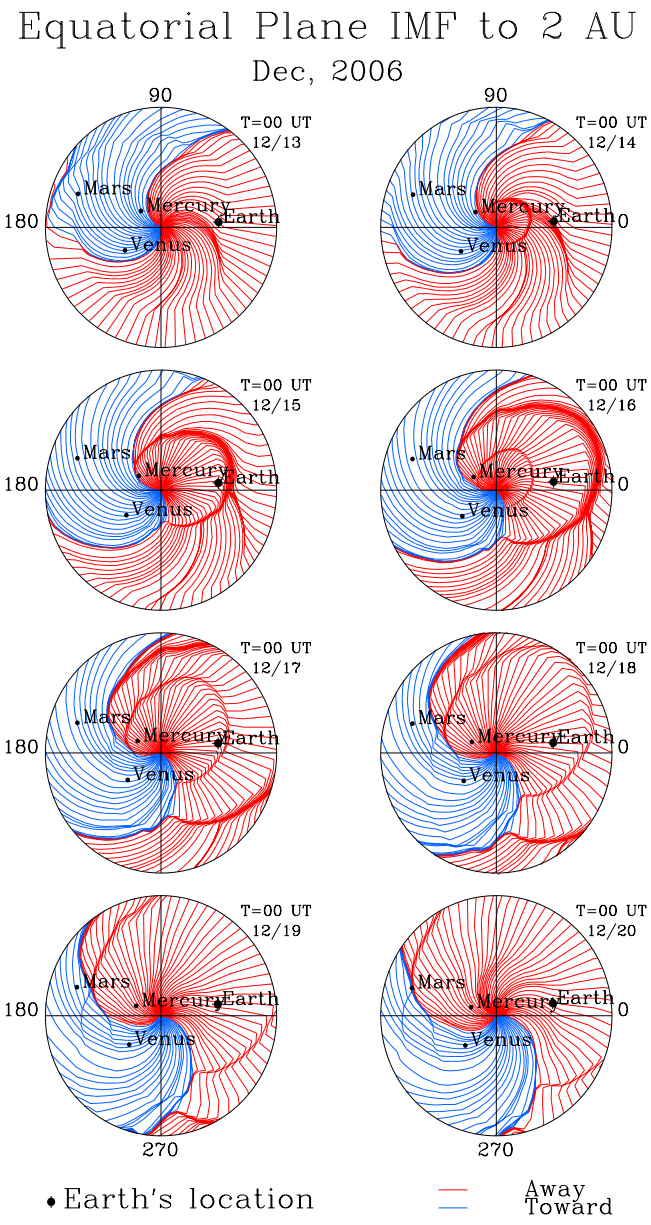

Figure 6. HAFv.2 simulation of disturbed IMF field lines in the ecliptic plane to 2 AU from 0000 UT on 13 December 2006 to 0000 UT on 20 December 2006 following flares 3 and 4. Shocks 3 and 4 are clearly indicated, with the latter following the former shock until the interaction at their flanks on 19 December 2006. The frames have a 12 h cadence.

Analyser) and the ASPERA/ELS (Electron Spectrometer). IMA measures the main ion components (H^+, H_2^+, He^+, and O^+) in the energy range 0.01–36 keV/q and the group of molecular ions from 20 to 80 amu/q in the energy range 100 eV – 40 keV/q. This instrument has an instantaneous field of view of 4.6° × 360° and electrostatic sweeping provides elevation (±45°) coverage. ELS is a spherical top hat electrostatic analyzer and collimator system that operates in the energy range 1 eV–20 keV and features a 4° × 360° field of view divided into sixteen 22.5° sectors. The intrinsic energy resolution ΔE/E is 8%. The energy sweep takes 4 s, during which time the ELS samples 128 energy levels. For further details see *Barabash et al.* [2007]. ASPERA-3 aboard MEX typically records data close to the Martian bow shock (BS) in 3–4 h intervals. ASPERA-4 on VEX makes observations 60 min before and after the inbound and outbound Venusian BS crossings. Since VEX only observes at pericenter, there is a data gap of ∼20 h between its observation sets.

[40] Figure 5 and its animated version (which is available on request) both show that the HAFv.2 model predicts the arrival of composite shock S1-S2 at Venus between 0300 and 0500 UT on 8 December 2006. There was a gap in the VEX ASPERA-4 observations from 1000 UT on 7 December to 0530 UT on 8 December, and the predicted shock was not observed in those data recorded thereafter. However, SEPs were detected simultaneously at both Venus and Mars in VEX/MEX data from 6 December at <0530 UT for some 3 d, i.e., until the interplanetary field entered an away sector. It is noted in this regard that although the ASPERA experiment is not designed to detect energetic protons, both IMA and ELS are capable of detecting high-dose radiation (X-ray, gamma-ray, or MeV ions) through recording a high incidence of uniform background counts. This is because such radiation can penetrate through the aluminum wall of the instrument and impact on the microchannel plate. The long duration of the background counts detected in December 2006, as well as their uniformity in all channels and from all measurement directions, indicates that they were due to particle rather than to electromagnetic radiation. See also *Futaana et al.* [2008]. The frames of Figure 5 starting at 0000 UT, 6 December, indicate that there was a COB point connection from shock S1 to both Venus and Mars. The times of the SEPs at both planets are discussed by *Futaana et al.* [2008]. These authors also show the occurrence of an ESP flux maximum at Venus at 0900 UT on 7 December, thereby suggesting the arrival of composite shock S1-S2. A comparison of measured and predicted shock arrival times is made in Table 3 for Venus, Mars, and Earth. Later frames in Figure 5 indicate that the eastern flank of shock S1-S2 decayed to an MHD wave after passing Venus. Thus, the nonobservation in the available data of a shock at Mars provides in this context another favorable indication of the success of the HAFv.2 model in predicting in this case a "correct null." (The interested reader is referred to *McKenna-Lawlor et al.* [2006] for definitions of hits, "misses," "false alarms," and correct nulls.)

[41] Figure 6 shows the expansion of simulated shocks S3 and S4 around the Sun. Like their predecessors, S1-S2, S3, and S4 were probably very weak along their far western flanks in the vicinity of Mercury. The simulation suggests very clearly that S3 and S4 decayed to MHD waves on both their eastern and western flanks and thus they never reached Venus. However, by the time the western flanks of shocks S3 and S4 attained the larger distance of Mars, S4 had caught up with, and can thus be expected to have interacted with, S3. The resultant shock was predicted to reach Mars at ∼0000 UT on 20 December 2006 at about the same time as the arrival of an IMF sector boundary (Figure 6). No magnetometer data are available to validate this latter prediction.

[42] It is worth noting that a slight deviation from symmetry and smoothness with respect to the shock shapes in the ecliptic plane is visible in both Figures 5 and 6. These

Table 3. Comparison of Predicted and Observed Shock Arrivals at Venus and Mars[a]

Event	FF	Predicted Arrival Year	Month	Day	Mars, UT	Venus, UT	Observed at Mars (Date and Time)	ΔT, h	TT, h	Observed at Venus (Date and Time)	ΔT, h	TT, h
1	663	2006	12	8	MHD[b]	Int.[c]	...	cn[d]	...	...	Int.	...
2	664	2006	12	8	MHD[b]	0300–0500	...	cn[d]	...	7 Dec. at 0900 UT[f]	19	14
3	665	2006	12	20	0000	Int.[c]	...	Int.[c]	...	...	cn[d]	...
4	666	2006	12	20	0000	MHD[b]	between 19 Dec. at 2345 UT and 20 Dec. at 0350 UT[e]	<4	122	...	cn[d]	...

[a]FF, fearless forecast number (see text); ΔT, shock arrival time predicted by HAFv.2 minus observed arrival time; TT, shock arrival time minus start time of metric type II burst.
[b]MHD, shock decays to an MHD wave.
[c]Int., shock interacts and combines with following event to form one wave.
[d]Here cn is correct null (no shock predicted and none observed).
[e]Inferred from a change in ion heating during the data gap (see Figure 7).
[f]Inferred from ion counts recorded in ASPERA-4 data [*Futaana et al.*, 2008].

deviations are caused by shock incursion into nonuniform regions in the upstreamflow [see, e.g., *Dryer et al.*, 2004; *Manchester et al.*, 2004, 2005]. In the former study, as in the present case, an ambient solar wind based on the most recently obtained solar magnetograms was utilized. In the latter case a nominal bimodal solar wind was inferred from earlier Ulysses observations. In both approaches, it can be inferred that preceding ICME and shock disturbances would lead, both within and outside the ecliptic plane, to shape distortion effects for ensuing shocks [*Dryer et al.*, 2001; *Sun et al.*, 2003].

[43] Figure 7 presents the data recorded by ASPERA-3/IMA. From top to bottom, Figure 7 shows the positions of the MEX spacecraft in a cylindrical coordinate system with, below, ion spectrograms recorded on 19–20 December 2006. Because of telemetry limitations, plasma data were recorded only in the close Martian environment (i.e., before 2345 UT on 19 December and after 0350 UT on 20 December). As indicated in Figure 7 by the label BS, the Martian bow shock was traversed by MEX at 2324 UT and, after that, MEX entered the solar wind. After 4 h, MEX again reached the Martian bow shock at 0424 UT on 20 December. Even though we do not have plasma data between the latter times, it can be seen that the ion distribution changed in the interim such that the ions recorded were significantly heated within the preceding 4 h. On the following day (not shown) the solar wind had reverted to being a cool beam. Since heating of the solar

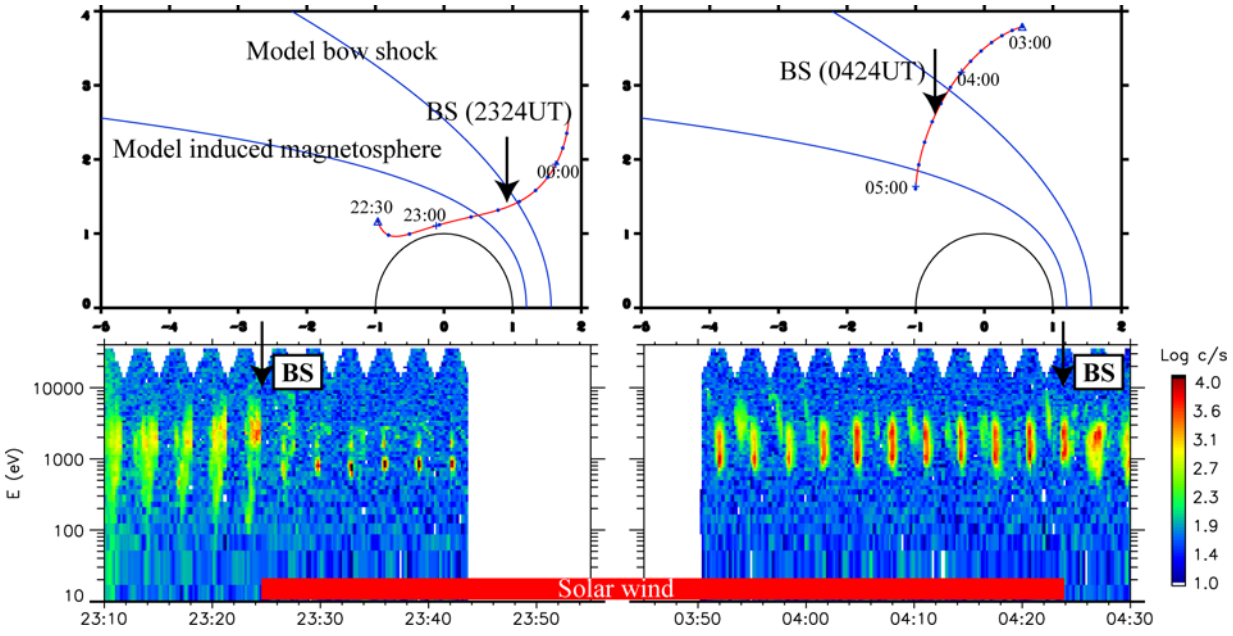

Figure 7. (top) Positions of MEX/ASPERA-3 in a cylindrical co-ordinate system with (bottom) IMA ion spectrograms. There are no data between 2345 UT on 19 December and 0350 UT on 20 December. Crossings by MEX of the Martian bow shock are indicated by BS (at 2324 UT on 19 December and 0424 UT on 20 December). Between these crossings MEX was in the solar wind (indicated by a solid bar). See the text for further information.

wind coincided with the predicted arrival time of composite shock S3-S4, we infer that the heating observed was likely to have been caused by the passage of this shock.

4. Concluding Remarks

[44] The 3-D HAFv.2 solar wind model has previously been shown to provide useful real time predictions of solar-generated IP shock arrivals at Earth [see, e.g., *Fry et al.*, 2003; *McKenna-Lawlor et al.*, 2006]. The latter workers identified a RMS error of ±11 h for successful hits (considering a total of 421 events of the type discussed here) during the rising and maximum phases of solar cycle 23 (from February 1997 to August 2002). They also considered the implications of using various arbitrarily chosen "windows" (such as ±24 h, ±12 h, etc.) for shock arrival hits. It is noted that the RMS error mentioned above has not yet been evaluated for the declining phase of cycle 23.

[45] The HAFv.2 model used here with respect to inner planetary "targets of opportunity" both during and after the X class flares and CMEs of 5, 6, 13, and 14 December 2006 demonstrate how HAFv.2 (or any other 3-D model) can be tested for prediction validation. It was found in the present case that in every instance the HAFv.2 model provided predictive hits at Earth well within the ±11 h metric noted above.

[46] A prediction of HAFv.2 was that composite shock S1-S2 would arrive at Venus on 8 December at ~0500 UT. Observations at Venus made by ASPERA-4 showed the occurrence of an ESP flux maximum at Venus at 0900 UT, on 7 December, thereby suggesting the arrival of composite shock S1-S2 approximately 19 h early with respect to the model prediction. No statistics are yet available to establish a RMS error with regard to shock arrivals at Venus. However, since interplanetary circumstances can influence whether shocks are accelerated/decelerated during their propagation through the heliosphere, the enhancement detected at 0900 UT on 7 December represents a good candidate for the expected composite shock. The nonobservation in the available data of composite shock S1-S2 at Mars is in accord with a prediction of HAFv.2 that the shock decayed to an MHD wave after passing Venus.

[47] HAFv.2 predictions when compared with in situ measurements made at Mars by MEX/ASPERA-3 suggest the possible arrival signature of shock S3-S4 in the data of 20 December 2006. This is in accord with a result previously obtained by *McKenna-Lawlor et al.* [2005] who demonstrated, using HAFv.2, that shocks associated with four major solar flares were predicted by the model to arrive at Mars at times that were appropriate to explain solar energetic particle events recorded in situ at the planet by the experiments SLED and LET aboard Phobos-2 in March 1989 (error approximately ±12 h). In the present case, the visualization in ecliptic plane plots of the time varying IMF connections between shocks S1 and S2 prior to their arrival at Venus (as indicated in Figure 6), suggests the future fruitful use of SEP flux and fluence in predictive analyses (such as the method described by *Aran et al.* [2007] in respect of its application to the particle set recorded by LET aboard Phobos-2 in March 1989).

[48] The HAFv.2 modeling of shocks S1 and S2 suggests a possible scenario for the physical process responsible for delivering to Earth "unusual" prompt and gradual SEPs during the December activity from far eastern solar flare locations (namely ongoing connectivity with Earth along the IMF lines of the Parker spiral from the western flank of strong composite shock S1-S2 as soon as it started to expand around the Sun). We tentatively infer in this regard, that the wave imaged by GOES 12/SXI moving in the low corona across the visible disk, which was also seen briefly over the east limb following the first flare (as noted by Steven Hill (private communication, 2007)) is in accord with the simulated behavior of shock S1. Similarly, we infer that the extensive associated Hα Morton wave reported by the National Solar Observatory supported, via its skirt role, the simulated behavior of IP shock S2 (Figure 6) before it merged with shock S1. Shock expansion around a spherical object is common in the field of hypersonic fluid mechanics [see, e.g., *Dryer et al.*, 1967]. Also, this process recently gained, in the solar context, substantial physical support (anisotropic wave and shock buildup) via a 3-D MHD simulation of a wave and associated CME recorded by SOHO's Extreme Ultraviolet Imaging Telescope that followed the well known solar event of 12 May 1997 [*Wu et al.*, 2001]. It is stressed that, while in the case of the activity of 5–6 December the modeling of shocks S1 and S2 suggest a scenario for delivering unusual SEPs from far eastern flare locations, no detailed physical explanation of the pertaining mechanism is as yet available to support this possibility.

[49] The present results indicate the predictive usefulness of a model such as HAFv.2 even in circumstances when Earth and Mars are located on opposite sides of the Sun. We did not infer that Flares 3 and 4 were strong enough to exhibit the degree of shock expansion indicated for Flare 2. Thus, we deem it to be unlikely that shock S3, shock S4, or even composite shock S3-S4 had sufficient strength to reach Mercury. We deduce, however, that a need for essentially continuous multipoint monitoring by future spacecraft at Earth and at the inner planets is demonstrated by our benchmarking experiment. Also that a definitive validation of predictive 3-D solar wind models at the inner planets will require continuous particle and magnetic field observations at these locations. Finally, we recommend that parallel efforts be made during different phases of the solar cycle to intercompare 3-D models during both quiet and disturbed periods.

[50] **Acknowledgments.** We thank the space weather forecasters at the U.S. Air Force Weather Agency (AFWA) and at the NOAA Space Environment Center (SEC) for their cooperation. We also thank the OSPAN project of NSO/AURA/NSF and the U.S. Air Force Research Laboratory for permission to use information (see text) on the Hα Moreton wave accompanying flare 2. OSPAN is funded and operated by USAF/AFRL in collaboration with the National Solar Observatory, Sunspot, New Mexico. Thanks are also extended to the STEREO/IMPACT Principal Investigator, Janet Luhmann, and her team for their immediate posting of energetic particle flux and magnetic field data on their website http://sprg.ssl.berkeley.edu/impact/events/IMPACTNews_curr.html. These data support the ACE level 1 data shown in Figure 3. The STEREO/WAVES data used here are produced by an international consortium of the Naval Research Laboratory (United States), Lockheed Martin Solar and Astrophysics Lab (United States), NASA Goddard Space Flight Center (United States), Rutherford Appleton Laboratory (United Kingdom), University of Birmingham (United Kingdom), Max-Planck-Institut für Sonnensystemforschung(Germany), Centre Spatiale de Liege (Belgium), Institut d'Optique Théorique et Appliqueé (France), and Institut d'Astrophysique Spatiale (France). The IRF participants thank the space agencies, departments, and institutes hosting those international efforts which have supported the ASPERA-3 and ASPERA-4 experiments on ESA's Mars Express and Venus Express missions. S.M.-L. thanks Enterprise Ireland for support concerning this

study. M.D. expresses his appreciation to NOAA/SEC for their hospitality during his emeritus tenure. K.Ke. expresses appreciation of Hungarian National grant OTKA-T-034566, and K.Ku. acknowledges support from the Slovak VEGA Grant Agency (project 4064). The authors thank the two reviewers for their constructive comments and suggestions.

[51] Amitava Bhattacharjee thanks Stephen Kahler and Merav Opher for their assistance in evaluating this manuscript.

References

Akasofu, S.-I., and C. D. Fry (1986), A first generation numerical geomagnetic storm prediction scheme, *Planet. Space Sci.*, *34*, 77–92, doi:10.1016/0032-0633(86)90105-4.

Aran, A., B. Sanahuja, and D. Lario (2006), Fluxes and fluences of SEP events derived from SOLPENCO, *Adv. Space Res.*, *37*(6), 1240–1246, doi:10.1016/j.asr.2005.09.019.

Aran, A., D. Lario, B. Sanahuja, R. G. Marsden, M. Dryer, C. D. Fry, and S. M. P. McKenna-Lawlor (2007), Modeling and forecasting solar energetic particle events at Mars: The event on 6 March 1989, *Astron. Astrophys.*, *469*, doi:10.1051/0004-6361:20077233.

Arge, C. N., and V. Pizzo (2000), Improvement in the prediction of solar wind conditions using near-real time solar magnetic field updates, *J. Geophys. Res.*, *105*, 10,465–10,479.

Barabash, S., et al. (2007), The Analyzer of Space Plasmas and Energetic Atoms (ASPERA-3) for the Mars Express mission, *Space Sci. Rev.*, *126*, 113–164, doi:10.1007/s11214-006-9124-8.

Cohen, C. M. S. (2006), Observations of energetic storm particles: An overview, in *Solar Eruptions and Energetic Particles*, edited by N. Gopalswamy, R. Mewaldt, and T. Torsti, *Geophys. Monogr. Ser.* vol. 165, pp. 275–282, AGU, Washington, D. C.

Detman, T. R., Z. Smith, M. Dryer, C. D. Fry, C. N. Arge, and V. J. Pizzo (2006), A hybrid heliospheric modeling system: Background solar wind, *J. Geophys. Res.*, *111*, A07102, doi:10.1029/2005JA011430.

Dryer, M. (1998), Multi-dimensional MHD simulation of solar-generated disturbances: Space weather forecasting of geomagnetic storms, *AIAA J.*, *36*(3), 365–370.

Dryer, M. (2007), Space weather simulations in 3-D MHD from the Sun to Earth and beyond to 100 AU: A modeler's perspective of the present state of the art, *Asian J. Phys.*, *16*, 122–146.

Dryer, M., D. L. Merritt, and P. M. Aronson (1967), Interaction of a plasma cloud with the Earth's magnetosphere, *J. Geophys. Res.*, *72*, 2955–2961.

Dryer, M., C.-C. Wu, and Z. K. Smith (1997), Three-dimensional MHD simulation of the April 14, 1994, interplanetary coronal mass ejection and its propagation to Earth and Ulysses, *J. Geophys. Res.*, *102*, 14065–14074, doi:10.1029/97JA00872.

Dryer, M., C. D. Fry, W. Sun, C. S. Deehr, Z. Smith, S.-I. Akasofu, and M. D. Andrews (2001), Prediction in real-time of the 2000 July 14 heliospheric shock wave and its companions during the "Bastille" epoch, *Sol. Phys.*, *204*, 265–284, doi:10.1023/A:1014200719867.

Dryer, M., C. D. Fry, W. Sun, C. S. Deehr, and S.-I. Akasofu (2004), Real-time predictions of interplanetary shock arrivals at L1 during the "Halloween 2003" epoch, *Space Weather*, *2*, S09001, doi:10.1029/2004SW000087.

Fry, C. D. (1985). The three-dimensional geometry of the heliosphere: Quiet time and disturbed periods, Ph.D. dissertation, Univ. of Alaska, Fairbanks.

Fry, C. D., W. Sun, C. S. Deehr, M. Dryer, Z. Smith, S.-I. Akasofu, M. Tokumaru, and M. Kojima (2001), Improvements to the HAF solar wind model for space weather predictions, *J. Geophys. Res.*, *106*, 20,985–21,001, doi:10.1029/2000JA000220.

Fry, C. D., M. Dryer, C. S. Deehr, W. Sun, S.-I. Akasofu, and Z. Smith (2003), Forecasting solar wind structures and shock arrival times using an ensemble of models, *J. Geophys. Res.*, *108*(A2), 1070, doi:10.1029/2002JA009474.

Fry, C. D., M. Dryer, W. Sun, T. R. Detman, Z. Smith, C. S. Deehr, C.-C. Wu, S.-I. Akasofu, and D. Berdichevsky (2004), Solar observation-based model for multi-day predictions of interplanetary shock and CME arrivals at Earth, *IEEE Trans. Plasma Sci.*, *32*(4), 1489–1497.

Fry, C. D., M. Dryer, W. Sun, C. S. Deehr, Z. Smith, A. Aran, D. Lario, B. Sanahuja, T. R. Detman, and S.-I. Akasofu (2005), Key links in space weather: Forecasting solar-generated shocks and proton acceleration, *AIAA J.*, *43*(5), 987–993, doi:10.2514/1.11470.

Fry, C. D., T. R. Detman, M. Dryer, Z. Smith, W. Sun, C. S. Deehr, S.-I. Akasofu, C.-C. Wu, and S. McKenna-Lawlor (2007), Real-time solar wind forecasting capabilities and challenges, *J. Atmos. Sol. Terr. Phys.*, *69*, 109–115, doi:10.1016/j.jastp.2006.07.024.

Futaana, Y., et al. (2008), Mars Express and Venus Express multi-point observations of geoeffective solar flare events in December 2006, *Planet. Space Sci.*, doi:10.1016/j.pss.2007.10.014, in-press.

Gabriel, S. (2006), The solar energetic particle environment: How to transition from science to International Standard Models, paper presented at 36th Committee on Space Research Assembly, Committee on Space Research, Beijing.

Hakamada, K., and S.-I. Akasofu (1982), Simulation of three-dimensional solar wind disturbances and resulting geomagnetic storms, *Space Sci. Rev.*, *31*, 3–70, doi:10.1007/BF00349000.

Intriligator, D. S., W. Sun, M. Dryer, C. D. Fry, C. S. Deehr, and J. Intriligator (2005), From the Sun to the outer heliosphere: Modeling and analyses of the interplanetary propagation of the October/November (Halloween) 2003 solar events, *J. Geophys. Res.*, *110*(A9), A09S10, doi:10.1029/2004JA010939.

Intriligator, D. S., W. Sun, T. Detman, and M. Dryer, C. D. Fry, C. Deehr, and J. Intriligator (2006), Solar variability effects in the outer heliosphere and heliosheath, in *Physics of the Inner Heliosheath: Voyager Observations, Theory, and Future Prospects; 5th Annual IGPP International Astrophysics Conference*, *Am. Inst. Phys. Conf. Proc. Ser.*, vol. 858, edited by J. Heerikhuisen et al., pp. 64–70, Springer, New York.

Lario, D., B. Sanahuja, and A. M. Heras (1998), Energetic particle events: Efficiency of interplanetary shocks as 50 keV < E < 100 MeV proton accelerators, *Astrophys. J.*, *509*, 415–434, doi:10.1086/306461.

Manchester, W. B., IV, T. I. Gombosi, I. Roussev, D. L. De Zeeuw, I. V. Sokolov, K. G. Powell, and T. Toth (2004), Three-dimensional MHD simulation of a flux rope driven CME, *J. Geophys. Res.*, *109*, A01102, doi:10.1029/2002JA009672.

Manchester, W. B., IV, T. I. Gombosi, D. L. De Zeeuw, I. V. Sokolov, I. I. Roussev, and K. G. Powell (2005), Coronal mass ejection shock and sheath structures relevant to particle acceleration, *Astrophys. J.*, *622*, 1225–1239, doi:10.1086/427768.

McAllister, A. H., M. Dryer, P. McIntosh, H. Singer, and L. Weiss (1996), A large polar crown CME and a "problem" geomagnetic storm: April 14–23, 1994, *J. Geophys. Res.*, *101*, 13497–13515, doi:10.1029/96JA00510.

McKenna-Lawlor, S., M. Dryer, C. D. Fry, W. Sun, D. Lario, C. S. Deehr, B. Sanahuja, V. A. Afonin, M. I. Verigin, and G. A. Kotova (2005), Prediction of energetic particle radiation in the close Martian environment, *J. Geophys. Res.*, *110*, A03102, doi:10.1029/2004JA010587.

McKenna-Lawlor, S., M. Dryer, M. D. Kartalev, Z. Smith, C. D. Fry, W. Sun, C. S. Deehr, K. Kecskemety, and K. Kudela (2006), Near real-time predictions of the arrival at the earth of flare-generated shocks during solar cycle 23, *J. Geophys. Res.*, *111*, A11103, doi:10.1029/2005JA011162.

McKenna-Lawlor, S. M. P., M. Dryer, Z. Smith, K. Kecskemety, C. D. Fry, W. Sun, C. S. Deehr, D. Berdichevsky, K. Kudela, and G. Zastenker (2002), Arrival times of flare/HALO CME associated shocks at the Earth: Comparison of the predictions of three numerical models with these observations, *Ann. Geophys.*, *20*, 917–935.

Newkirk, G., Jr. (1961), Solar corona in active regions and the thermal origin of the slowly varying component of solar radiation, *Astrophys. J.*, *133*, 983–1013, doi:10.1086/147104.

Odstrcil, D., M. Dryer, and Z. Smith (1998), Numerical Simulation of March 1991 Interplanetary Disturbances (SOLTIP Interval 1), in *Advances in Solar Connection With Transient Interplanetary Phenomena; Proceedings of the Third SOLTIP Symposium*, edited by X. S. Feng, F. S. Wei, and M. Dryer, pp. 191–200, Int. Acad., Beijing.

Odstrcil, D., V. J. Pizzo, and C. N. Arge (2005), Propagation of the 12 May 1997 interplanetary coronal mass ejection in evolving solar wind structures, *J. Geophys. Res.*, *110*, A02106, doi:10.1029/2004JA010745.

Posner, A., N. A. Schwadron, D. J. McComas, E. C. Roelof, and A. B. Galvin (2004), Suprathermal ions ahead of interplanetary shocks: New observations and critical instrumentation required for future space weather monitoring, *Space Weather*, *2*, S10004, doi:10.1029/2004SW000079.

Smart, D. F., M. A. Shea, W. R. Barron, and M. Dryer (1984), A simplified technique for estimating the arrival time of solar flare-initiated shocks, in *Proceedings of STIP Workshop on Solar/Interplanetary Intervals, August 4–6, 1982, Maynooth, Ireland*, edited by M. A. Shea, D. F. Smart, and S. McKenna-Lawlor, pp. 139–156, Book Crafters, Chelsea, Mich.

Smith, Z. (2002). Demonstration of method to evaluate in the operational environment space weather models that predict shock arrivals and geomagnetic disturbances using solar and interplanetary data for input, in *Proceedings of the 10th European Solar Physics Meeting "Solar Variability from Core to Outer Frontiers"*, edited by A. Wilson, pp. 205–209, Eur. Space Agency, Paris.

Smith, Z., W. Murtagh, T. Detman, M. Dryer, C. D. Fry, and C.-C. Wu (2003), Study of Solar-Based Inputs into Space Weather Models that Predict Interplanetary Shock Arrivals at Earth, in *Proceedings of International Solar Cycle 2003 Symposium, "Solar Variability as an Input to the Earth's Environment"*, edited by A. Wilson, pp. 547–552, Eur. Space Agency, Paris.

Smith, Z., T. Detman, M. Dryer, C. D. Fry, C.-C. Wu, W. Sun, and C. S. Deehr (2004), A verification method for space weather models using solar data to predict arrivals of interplanetary shocks at Earth, *IEEE Trans. Plasma Phys.*, *32*(4), 1498–1505.

Smith, Z., M. Dryer, and C. D. Fry (2005), Determining shock velocities for inputs to Sun-to-Earth models from radio and coronagraph data, *Space Weather*, *3*(7), S07002, doi:10.1029/2004SW000136.

Sun, W., S.-I. Akasofu, Z. K. Smith, and M. Dryer (1985), Calibration of the kinematic method of studying solar wind disturbances on the basis of a one-dimensional MHD solution and a simulation study of the heliosphere between November 22 and December 6, 1977, *Planet. Space Sci.*, *33*, 933–943, doi:10.1016/0032-0633(85)90107-2.

Sun, W., M. Dryer, C. D. Fry, C. S. Deehr, Z. Smith, S.-I. Akasofu, M. D. Kartalev, and K. G. Grigorov (2002a), Evaluation of solar type ii radio burst estimates of initial solar wind shock speed using a kinematic model of the solar wind on the April 2001 solar event swarm, *Geophys. Res. Lett.*, *29*(8), 1171, doi:10.1029/2001GL013659.

Sun, W., M. Dryer, C. D. Fry, C. S. Deehr, Z. Smith, S.-I. Akasofu, M. D. Kartalev, and K. G. Grigorov (2002b), Real-time forecasting of ICME shock arrivals at L1 during the "April Fool's Day" Epoch: 28 March–21 April 2001, *Ann. Geophys.*, *20*, 937–945.

Sun, W., C. S. Deehr, C. D. Fry, M. Dryer, Z. Smith, and S.-I. Akasofu (2003), Plane-of-sky simulations of interplanetary shock waves, *Geophys. Res. Lett.*, *30*(20), 2044, doi:10.1029/2003GL017574.

Tsurutani, B., S. T. Wu, T. X. Zhang, and M. Dryer (2003), Coronal mass ejection (CME) induced shock formation, propagation, and some temporally and spatially-developing shock parameters relevant to particle energization, *Astron. Astrophys.*, *412*, 293–304, doi:10.1051/0004-6361:20031413.

Vandegriff, J., K. Wagstaff, G. Ho, and J. Plauger (2005), Forecasting space weather: Predicting interplanetary shocks using neutral networks, *Adv. Space Res.*, *36*(12), 2323–2327, doi:10.1016/j.asr.2004.09.022.

Wang, Y. M., and N. R. Sheeley (1990), Solar wind speed and coronal flux-tube expansion, *Astrophys. J.*, *355*, 726–732, doi:10.1086/168805.

Wu, C.-C., C. D. Fry, D. Berdichevsky, M. Dryer, Z. Smith, and T. Detman (2005), Predicting the arrival time of shock passages at Earth, *Sol. Phys.*, *227*(2), 371–386, doi:10.1007/s11207-005-1213-4.

Wu, C.-C., X. S. Feng, S. T. Wu, M. Dryer, and C. D. Fry (2006), Effects of the interaction and evolution of interplanetary shocks on "background" solar wind speeds, *J. Geophys. Res.*, *111*, A12104, doi:10.1029/2006JA011615.

Wu, C.-C., C. D. Fry, S. T. Wu, M. Dryer, and K. Liou (2007), Three-dimensional global simulation of interplanetary coronal mass ejection propagation from the Sun to the heliosphere: Solar event of 12 May 1997, *J. Geophys. Res.*, *112*, A09104, doi:10.1029/2006JA012211.

Wu, S. T., H. Zheng, S. Wang, B. J. Thompson, S. P. Plunkett, X. P. Xhao, and M. Dryer (2001), Three-dimensional numerical simulation of MHD waves observed by the Extreme Ultraviolet Imaging Telescope, *J. Geophys. Res.*, *106*, 25,089–25,102, doi:10.1029/2000JA000447.

J. Balaz and K. Kudela, Institute of Experimental Physics, Watsonova 47, 040 01 Kosice, Slovakia.

S. Barabash, Y. Futaana, R. Lundin, and M. Yamauchi, Swedish Institute of Space Physics, Box 812, SE-981 28, Kiruna, Sweden.

W. R. Courtney, Space Operations, U.S. Air Force Weather Agency, Offutt Air Force Base, Omaha, NE 68113, USA.

C. S. Deehr and W. Sun, Geophysical Institute, University of Alaska, 903 Koyukuk Drive, Fairbanks, AK 99775, USA.

M. Dryer and Z. K. Smith, Space Environment Center, Space Weather Predictions Centre, National Weather Agency, 325 Broadway, Boulder, CO 80305, USA.

C. D. Fry, Exploration Physics International, Inc., 6275 University Drive NW, Suite 37-105, Huntsville, AL 35806, USA.

D. S. Intriligator, Carmel Research Center, P.O. Box 1732, Santa Monica, CA 90406, USA.

K. Kecskemety, Research Institute for Particle and Nuclear Physics, Központi Fizikai Kutató Intézet, Konkoly Thege Miklós út 29-33, H-1121 Budapest, Hungary.

S. M. P. McKenna-Lawlor, Space Technology Ireland, National University of Ireland, Maynooth, Ireland. (stil@nuim.ie)